

# SPECIAL ASPECTS OF FLIGHT DYNAMICS OF A REUSABLE CRYOGENIC BOOSTER STAGE

Josef Klevanski <sup>(1)</sup>, Martin Sippel <sup>(2)</sup>,

<sup>(1)</sup> *Space Launcher Systems Analysis (SART), DLR, Linder Hoehe, 51147 Cologne, Germany,  
Email: [josef.klevanski@dlr.de](mailto:josef.klevanski@dlr.de)*

<sup>(2)</sup> *Space Launcher Systems Analysis (SART), DLR, Linder Hoehe, 51147 Cologne, Germany,  
Email: [martin.sippel@dlr.de](mailto:martin.sippel@dlr.de)*

## ABSTRACT

The semi-reusable Space Transportation System (STS) investigated in the German ASTRA research program consists of two reusable winged liquid fly-back booster stages called LFBB attached to the expendable Ariane 5 core at an upgraded technology level. The focus of the presented study is the in-depth research of the special aspects of flight dynamics of a LFBB in all flight phases and especially the investigation of the trimmability, stability and controllability.

The LFBB-layout is developed under consideration of tight structural and geometrical constraints of using European cryogenic rocket engine technology [1].

These design conditions result in the special LFBB layout features, such as its large diameter fuselage and a forward position of the air-breathing engines. The great variation in the location of the center of pressure for different Mach numbers caused by large diameter fuselage and a wide range of center of gravity position demand canards for trim and control purposes.

The aerodynamic investigation loop performed by the DLR Institute of Aerodynamics and Flow Technology in Braunschweig [2],[3] and in the DLR Wind Tunnel in Cologne [6] allowed optimizing the key features of the aerodynamical layout, such as the canards shape and the wing profile.

The main task of this study is the investigation of the longitudinal flight dynamics of the LFBB using the obtained aerodynamic data within a closed loop simulation taking into account rigid body equations of motion, control law and actuators by realistic assumption. This paper discusses the controllability of the whole STS during the ascent phase until separation including wind gust influence, guaranteeing of the structural constraints during re-entry phase and the trimmability and controllability of the LFBB during the cruise return flight.

The flight dynamics behavior of the LFBB is investigated for different center of gravity positions with reasonable margins.

## NOMENCLATURE

D	Drag	N
H	Altitude	m
L	Lift	N
M	Mach-Number	-
P	Thrust	kN
S	Distance	m
T	Throttle	-
V	Velocity	m/s
W	Weight	N
k, K	Control System Coefficients	
m	Mass	kg, t
n	Load Factor	-

q	Dynamic Pressure	Pa
$\alpha$	Angle Of Attack	Rad, deg
$\delta_c$	Control Surface Deflection	Rad, deg
$\gamma$	Flight Path Angle	Rad, deg
$\varepsilon$	Part Signal Of Control	
$\sigma$	Bank Angle	Rad, deg
$\nu$	Pitch Angle	Rad, deg
$\omega$	Pitch Rate	Rad/s, deg/s
$\psi$	Azimuth	Rad, deg
$\lambda$	Longitude	Rad, deg
$\varphi$	Latitude	Rad, deg

## SUBSCRIPTS, ABBREVIATIONS

2 DOF	Two Degrees Of Freedom
3 DOF	Three Degrees Of Freedom
GLOW	Gross Lift-Off Weight
LFBB	Liquid Fly-Back Booster
MECO	Main Engine Cut Off
RLV	Reusable Launch Vehicle
RCS	Reaction Control Systems
sep	Separation
STS	Space Transportation System
TVC	Thrust Vector Control

## 1 INTRODUCTION

The first objective of this flight dynamics analysis is the proof of the most important design data according to stability and controllability requirements such as:

- Aerodynamics and control surfaces efficiency
- Center of mass position
- Control laws functionality

The second objective is the proof of the safe operational range conditions for all flight phases:

- Ascent of the whole STS and staging
- Ballistic flight, reentry, cruise flight and landing

The considered semi-reusable Space Transportation System (STS) consists of two booster stages which are attached to the expendable core stage (*Figure 1*).

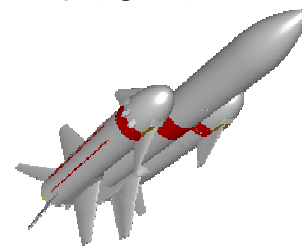


*Figure 1: Semi-reusable Space Transportation System*

The concept chosen for the LFBB which uses a LH2/LOX propellant combination for the main rocket motors (Ascent Phase) and LH2 as fuel for the air-breathing engines for the Cruise Return Flight Phase leads to the big volume of the propellant / oxidizer integral tanks. This results in a relatively big and long fuselage. The main delta wing is located aft of the integral tanks. Such layout is characterized by a variation in the location: of the center of pressure as a function of the Mach number and of the center of mass as a function of propellant consumption. This inevitably results in application of canards as main longitudinal trim and control surface. Specifics regarding the canards schema will be also discussed.

The whole flight segment of the LFBB can be divided in several most important flight phases (*Figure 2*):

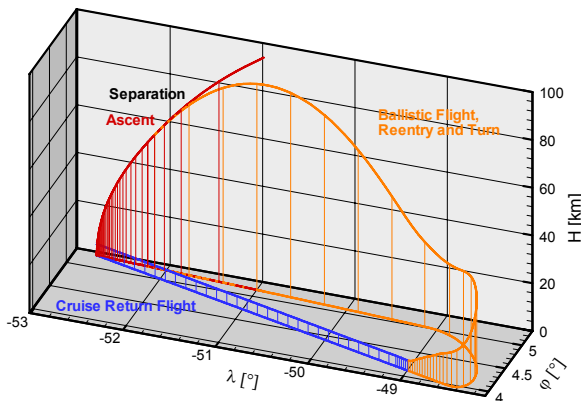


Figure 2: Flight Phases of RLV

- **Ascent Phase:**  
The flight from take-off with rocket motors propulsion up to the staging (LFBB separation)
- **Ballistic Phase:**  
The flight after separation up to re-entry into the dense atmosphere
- **Reentry and Turn Phase:**  
The leveling of the trajectory in the dense atmosphere and heading to the return azimuth
- **Return Cruise Flight Phase and Landing:**  
The atmospheric flight after turn back to the launch site with airbreathing engines propulsion.

All these flight phases differentiate essentially in aerodynamic characteristic/ flight dynamics behavior as well as in task of control system, control law and control means

## 2 MATHEMATICAL MODEL FOR SIMULATION

The unified modular mathematical model structure [4] based on the dynamical nonlinear equations of motion in CAUCHY-Form is used for stability and controllability investigations for all flight phases. Mathematical model includes in addition to the equations of motion the aerodynamic model, mass & inertia moment model, rocket engine model as well the mathematical model of the control system and TVC actuators.

### Flight dynamics model:

2DOF equations of motion with the flat Earth model are used for the simulation of the Ascent Phase whereas the 3DOF

equations with the ellipsoid Earth model are used for Ballistic Phase, Reentry and Turn Phase Return Cruise Flight Phase.

### Aerodynamics:

The aerodynamic coefficients for Drag, Lift and Momentum for the whole STS-configuration for the Ascent Phase are estimated by DLR program CAC v. 2.24 based on handbook methods as a function of the angle of attack and Mach number  $CL, CD; CM = f(M, \alpha)$ .

The aerodynamic coefficients for a single LFBB used for simulation for all flight phases after staging are calculated using CFD methods (TAU-Code for  $M \leq 2$ , HOTSOSE-Code for  $M > 2$ ) [2],[3]. The values obtained were confirmed by wind tunnel tests results [6]

### Mass and inertia model:

The following rigid body model is used:

$$m, I_{yy}, x_{cog}, z_{cog} = f(m_0, \dot{m}, t)$$

Vehicle mass values are derived from [1].

Propellant mass, CoG and inertia of wet launcher are based on formulas for cylindrical tanks, neglecting fluid dynamical effects. Linear interpolation of all values between initial and final state is used.

### Propulsion model:

Rocket motors thrust as a function of the specific impulse, mass flow and current altitude  $P = f(I_{sp}, \dot{m}, H)$  utilizes the Vulcain 3 engine data (S=35) for Ascent Phase.

The calculation of the air breathing engines data  $P = f(M, H, T)$  was made using the DLR program **abp** on basis of published data

### TVC:

Nozzle actuators modeled as first-order time-delay element with threshold of  $0.1^\circ$  and maximum deflection of nozzles of  $5.5^\circ$  Maximum gimbal velocity is limited to  $10^\circ/s$ .

The canards actuators are simulated as usual for the aircraft respecting the insensitivity zone.

## 3 ASCENT PHASE

In this section we discuss the flight of the STS which consists of two LFBBs and one central core stage. The control and trimming are carried out by the Thrust Vector Control (TVC) which performs simultaneous deflection of all main rocket motors of both LFBBs.

The main task of the attitude control system in this flight phase is to follow of the previously calculated optimal flight path and to compensate for all acting distortions such as altitude wind variations and wind gusts.

During the Ascent Phase control is provided from central core stage, and the control systems of the LFBBs function as sub-systems.

Especially intensive changes in the center of mass location and inertia moments occur during this flight phase as result of the propellant consumption. Severe changes in the center of pressure location occur as result of rapid Mach number increase. The dynamic pressure changes very rapidly too.

The closed loop control system follows the optimal ascent flight trajectory:

$$\delta_{TW} = k_{\omega_y} \cdot \omega_y + k_g \cdot \int (\mathcal{G}_{set} - \mathcal{G}_{act}) dt \quad (1)$$

All six booster engines are gimballed for control purposes

Wind is modeled according to GRAM-95: The Profile according to mean east-west wind for Jan 01 2010 (worst case orientation for launcher), is shown in *Figure 3*

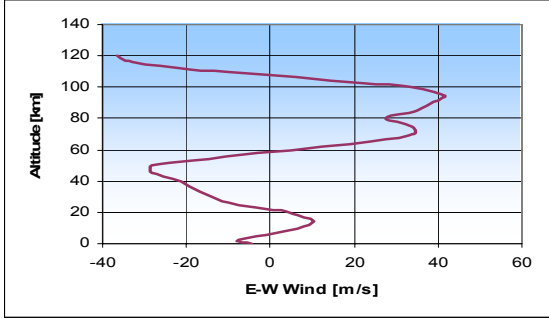


Figure 3 Wind profile for Ascent Simulation

The simulation was performed for a wind gust of 10 m/s at the 30<sup>th</sup> second for the Ascent Phase, where the product of the dynamic pressure and angle of attack,  $q \cdot \alpha$ , reaches its maximum (conservative assumption).



Figure 4: Load factors  $n_x$  and  $n_z$

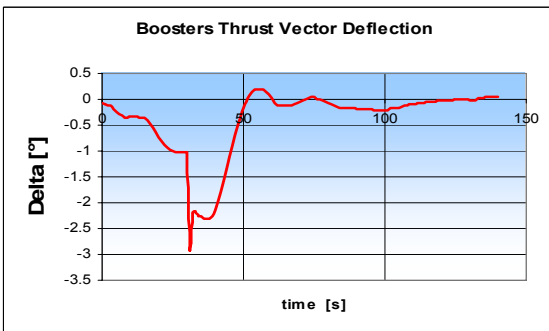


Figure 5: Thrust vector deflection  $\delta_{TVC}$

The results of the mathematical simulation shows that the influence of wind distortion on the STS, consisting of central core with two winged LFBBs with the big diameter fuselage is more intensive than by system with small wingless expendable boosters.

Nevertheless the chosen control law allows to compensate all distortions from variable wind profile and wind gust and to guarantee the necessary precision of the ascent trajectory.

#### 4 BALLISTICAL PHASE

After separation from the central core the Liquid Fly-Back Boosters continue the flight along a ballistic trajectory, reaching an altitude of ca. 90 km. The dynamic pressure in this flight phase is insignificant and the aerodynamic forces are small. Trim and control are provided by the Reaction Control Systems engines (RCS) located in the nose section of the fuselage. This schema is precise enough to provide the moment trim, the force trim is not necessary.

The main task of the control system in this flight phase is to provide the necessary angle of attack and roll angle before re-entry begins and to maintain these values.

The possibilities of the trajectory control in the ballistic part of the flight are highly restricted in any case. During this phase the control system provides stabilization and satisfies the flight limitations and constraints.

The corresponding part of the control law is:

$$\dot{\alpha}_{set} = K_{\alpha} \cdot (\alpha_{reentry} - \alpha_{cur}) \quad (2)$$

where  $\alpha_{set}$  is the assigned value of the angle of attack,  $\alpha_{cur}$  - is the current value of the angle of attack and  $K_{\alpha}$  is the control systems coefficient.

#### 5 RE-ENTRY GLIDE, DESCENT AND TURN

Until begin of the re-entry phase, the attitude control task is fulfilled at first via the RCS (Reaction Control Systems) as long as the dynamic pressure remains low. A gradual switching to aerodynamic control, as the dynamic pressure increases during re-entry, is then performed.

The feature specific to this flight phase is a very rapid change of Mach number and dynamic pressure. This results in intensive change in the values of angle of attack and the corresponding trim canards deflection. (*Figure 6, Figure 7*)

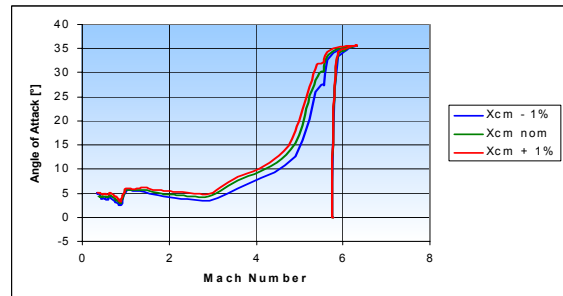


Figure 6: Angle of Attack as Mach number function

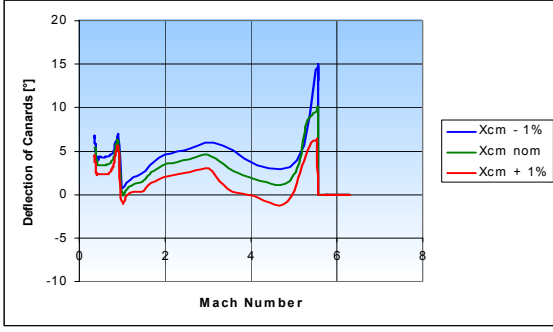


Figure 7: Trim Canards Deflection as Mach number function

During re-entry very important limitations must be respected: the normal g-load factor  $n_z \leq n_{z \text{ lim}}$ , the admissible dynamic pressure  $q \leq q_{\text{lim}}$  (the structure design stress limitations) and the heat flux limitations. Since the normal acceleration  $n_z$  will be determined by the aerodynamical data of the LFBB, as a function of the angle of attack, Mach number and dynamic pressure  $n_z = C_L(\alpha, M) \cdot q \cdot S_{\text{ref}} / m$  it is natural to entrust the control system with the limiting of its values via  $\alpha$  - angle of attack control. It is significant to note that normal acceleration  $n_z$  can be easily measured in real time with satisfactory precision.

However, the aerodynamic stability of the LFBB is very critical for the applied control law: the naturally stable booster still tries to reduce the angle of attack, therefore only a small risk to break the  $n_z$ -limitation exists even by moderate requirement for the control system. On the other hand, an unstable LFBB will demand a very high responsivity (running speed) of the closed loop control system.

That is to note, that the chosen aerodynamic canards schema has advantages in the responsivity of the LFBB with respect to the classic aircraft stabilizer/elevator schema: This is due to the fact that the first  $n_z$  - reaction to the canard deflection has the same sign as the  $n_z$  change resulting from an angle of attack change.

The control system uses the integral control law and applies during re-entry the following partial algorithm:

$$\text{if}(n_{z \text{ cur}} > n_{z \text{ lim}}):$$

$$\dot{\alpha}_{\text{set}} = K_{n_z} \cdot (n_{z \text{ lim}} - n_{z \text{ cur}}) \quad (3)$$

$$\text{if}(n_{z \text{ cur}} \leq n_{z \text{ lim}}): \quad \dot{\alpha}_{\text{set}} = 0$$

where  $\alpha_{\text{set}}$  is the assigned value of the angle of attack,  $n_{z \text{ lim}}$  - is the maximal admissible value of the normal acceleration,  $n_{z \text{ cur}}$  - is the current value of the normal acceleration and  $K_{n_z}$  is the control systems coefficient.

The angle of attack reduction results almost directly in the reduction of the normal acceleration. However, as the above described control law has a dynamic inaccuracy, the assigned value of the normal acceleration is chosen to be slightly below the stress limitation  $n_{z \text{ lim}}$ .

The necessary deflection of the control surface is:

$$\dot{\delta}_c = K_{\alpha} \cdot (\alpha_{\text{cur}} - \alpha_{\text{set}}) + K_{\omega_y} \cdot \omega_y \quad (4)$$

where  $\alpha_{\text{set}}$  is the assigned value of the angle of attack,  $\alpha_{\text{cur}}$  is the current value of the angle of attack,  $\omega_y$  is the pitch angle rate, and  $K_{\alpha_{\text{set}}}$ ,  $K_{\omega_y}$  are the control systems coefficients. This signal is used as an input signal by a simple mathematical model of the control surface actuator.

The typical re-entry history of  $\alpha$  and  $n_z$  is shown in Figure 8

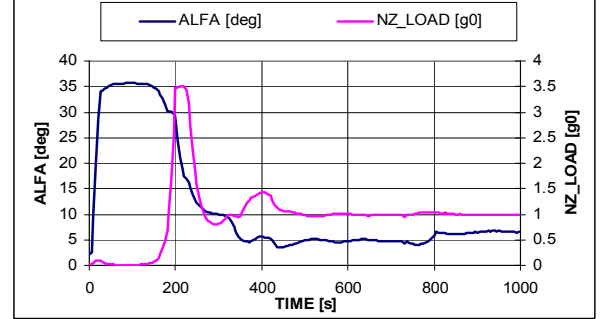


Figure 8: Angle of Attack and Dynamic Pressure Reentry History

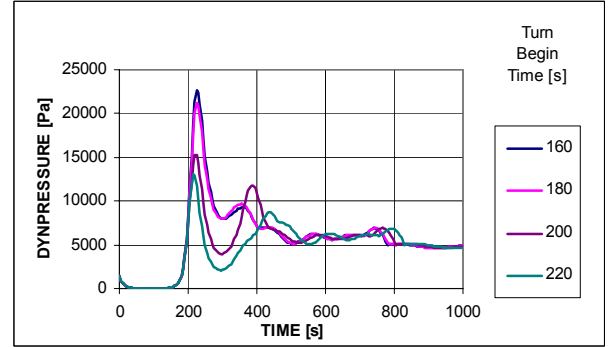


Figure 9: Dynamic Pressure Reentry Histories by Different Turn Begin Times

The dynamic pressure cannot be simultaneously directly controlled, but its peak values depend on the chosen turning time and on the limitation of the bank angle applied to the turn (Figure 9). The relatively small specific wing loading allows beginning of the turn maneuver simultaneously with re-entry.

On the one hand, an early turn begin can result in too high peak values of the dynamic pressure at re-entry while, on the other hand a late turn begin unnecessarily increases the return flight distance (s. Figure 10).

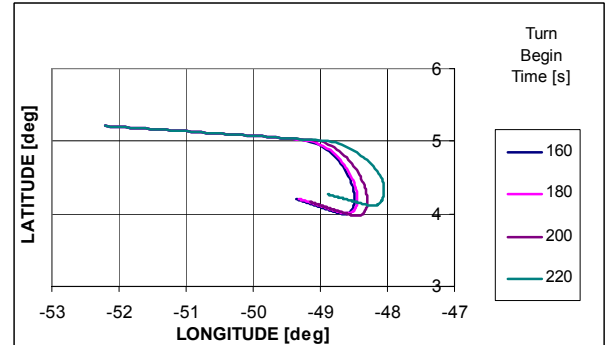


Figure 10: Turn Tracks by Different Turn Begin Times

This means that a compromise solution which satisfies the dynamic pressure limitation and at the same time provides the minimal return flight distance, can be properly found by performing variation at the time of turn begin.

The turn on the return course will be performed according to the following control law:

$$\begin{aligned} \dot{\sigma} &= K_{\psi} (\psi_{targ} - \psi_{cur}) + n_z \cdot \sin \sigma \\ |\sigma| &\leq \sigma_{max} \end{aligned} \quad (5)$$

After decreasing of the maximum normal acceleration and after transit through the maximum dynamic pressure the longitudinal channel of the control systems provides descent with the maximal lift-drag ratio until the rated return flight altitude.

## 6 RETURN CRUISE FLIGHT WITH AIR-BREATHING ENGINES

In the Return Cruise Flight Phase the main task of the control system is to maintain the flight along the along the shortest way to the target point with the minimal possible fuel consumption per range [5].

The navigation system continuously calculates the necessary value of the target azimuth that provides the shortest return flight route – the flight along the "orthodrome", a segment of the great circle. The attitude control system permanently maintains heading according to the following control law:

$$\begin{aligned} \dot{\sigma} &= K_{\psi} (\psi_{targ} - \psi_{cur}) + n_z \cdot \sin \sigma \\ |\sigma| &\leq \sigma_{max} \end{aligned} \quad (6)$$

The optimal flight conditions, which guarantee the minimal achievable fuel consumption per range  $H_{opt}, M_{opt} = f(m)$  will be set in the control system as the optimal flight profile.

During the return cruise flight this profile will be followed using the following integral control law:

$$\begin{aligned} \dot{\alpha}_{set} &= K_H \cdot (H_{opt} - H_{cur}) \\ \dot{T} &= K_T \cdot (M_{opt} - M_{cur}) \end{aligned} \quad (7)$$

where  $\alpha_{set}$  is the assigned angle of attack value,  $T$  is the assigned engine throttling,  $H_{opt} = f(m_{cur})$ ,  $M_{opt} = f(m_{cur})$  - are the optimal altitude and Mach number for the current mass value,  $H_{cur}, M_{cur}$  are current values of the of the altitude and Mach number respectively and  $K_H, K_T$  are the control systems coefficients.

Figure 11 and Figure 12 show the significant influence of the canards deflection and the center of gravity location on the longitudinal stability. The LFBB is in subsonic flight mode practically neutral up to slightly instable.

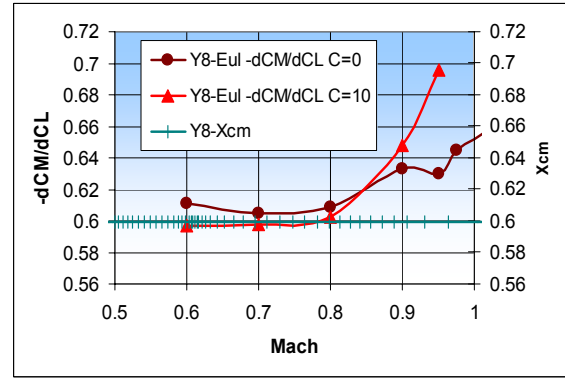


Figure 11: Influence of the Canards Deflection on the Stability.

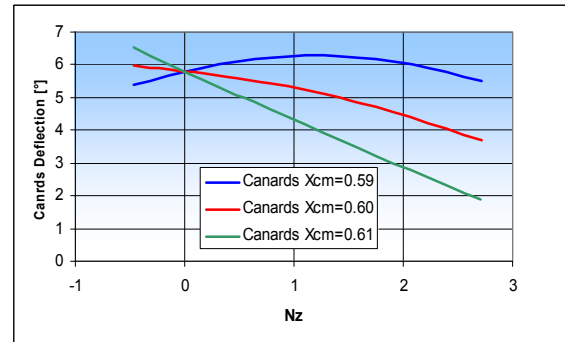


Figure 12: Influence of the COG-Location on the Stability.

It has to be noted, that the location of the air breathing engines in the upper nose section of the fuselage increases the necessary trim deflection of canards and has a negative influence on the landing leveling dynamics: By increasing of thrust the negative longitudinal moment appears (Figure 13). But this negative moment can be easily compensated by the control system, and the design advantages (compact and easy of access engine bay) prevail.

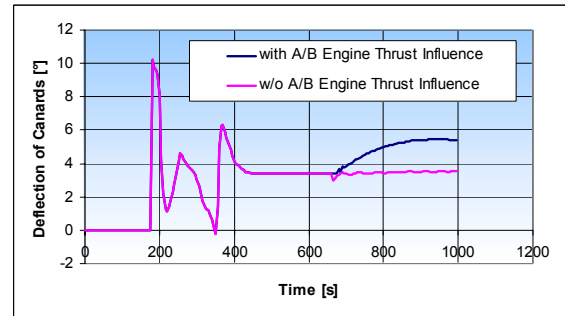


Figure 13: Influence of the Airbreathing Engines Thrust Vector on the Trim Deflection of Canards

The typical histories of the flight path angle  $\gamma$  and of the control surfaces deflection  $\delta_c$  for the vehicle, which is instable in the subsonic flight phase, are shown in the Figure 14.

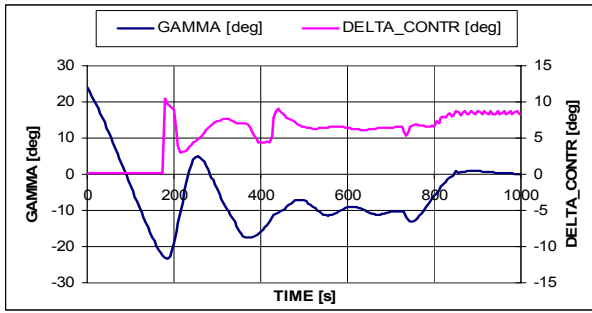


Figure 14: Pitch Angle and Control Surface Deflection History

The Cruise Flight Phase is a relatively long phase (about 1 hour). Therefore the gust and maneuvering envelopes were calculated under a very conservative assumption:  $CL_{max} = 0.6$ .

**GUST ENVELOPE** M=50000. S=347. G/S=1413.06  $CL_{max}=0.6$   $dCL/d\alpha|_{1/ra}$

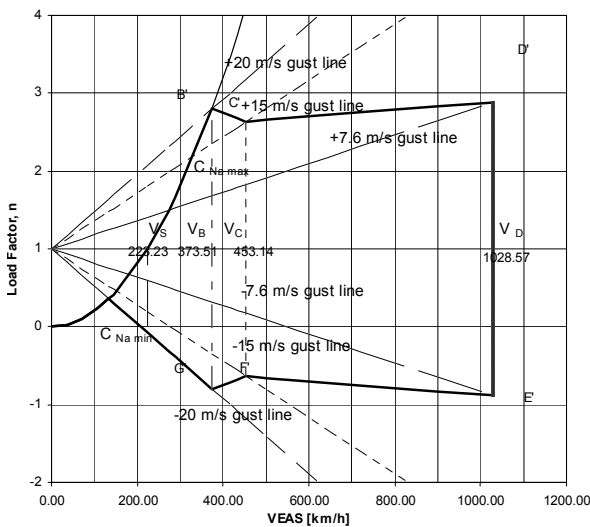


Figure 15: Gust Envelope

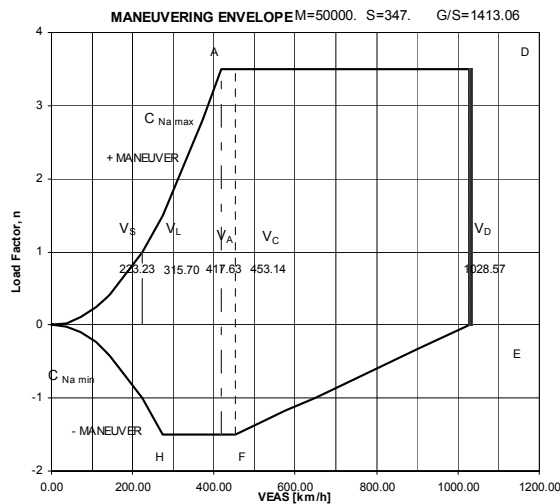


Figure 16: Maneuvering Envelope

Although the LFBB's cruise flight velocity is slower than recommended for civil transport aircraft by FAR-25, the stall and structure crash requirements are fulfilled.

## 7 CONCLUSIONS

- Controllability of the winged configuration during ascent flight by TVC can be proved.
- Aerodynamic Trimming & longitudinal Controllability of the reusable stage in the complete Descent flight regime including Reentry and Return Cruise Flight is achievable also with reasonable margins for the Center of Gravity.
- The longitudinal Stability in the subsonic return cruise flight can be provided by the automatic control system with a proper control law.
- Aspects of lateral Stability and Controllability have to be investigated in more detail in the next research phase.
- Safe operational range conditions for all Flight Phases can be proved.

## 8 REFERENCES

- [1] M. Sippel, J. Klevanski  
*Preliminary Definition of an Aerodynamic Configuration for a Reusable Booster Stage within Tight Geometric Constraints*. Fifth European Symposium on Aerothermodynamics for Space Vehicles, Cologne, November 2004
- [2] Th. Eggers:  
*Aerodynamic Design of an Ariane 5 Reusable Booster Stage*. Fifth European Symposium on Aerothermodynamics for Space Vehicles, Cologne, November 2004
- [3] Th. Eggers:  
*Longitudinal Stability and Trim of an Airane 5 Fly-Back Booster*. AIAA Paper 2003-7055, 2003
- [4] I. Klevanski, A. Herbertz, J. Kauffmann, V. Schmid.  
*Aspekte der Stabilität und Steuerbarkeit in der Flug- und Separationsphase unsymmetrischer Träger-Konfigurationen*. DGLR JT 2000
- [5] J. Klevanski, M. Sippel  
*Quasi-Optimal Control for the Reentry and Return Flight of an RLV*. 5th International Conference on Launcher Technology - Madrid 2003
- [6] F. Tarfeld  
*Comparison of two Liquid Fly-Back Booster Configurations based on Wind Tunnel Measurements*. Fifth European Symposium on Aerothermodynamics for Space Vehicles, Cologne, November 2004